# Intrinsic viscoelasticity in thin high-molecular-weight polymer films

Xiaoyuan Sheng,[1] Frédéric Wintzenrieth,[1,*] Katherine R. Thomas,[2,†] and Ullrich Steiner[1,‡]
[1]*Cavendish Laboratory, University of Cambridge, Cambridge CB3 0HE, United Kingdom*
[2]*Max-Planck Institute for Dynamics and Self-Organization, Am Fassberg 17, 37077 Göttingen, Germany*
(Received 7 October 2013; published 30 June 2014)

The rheology of 44–75-nm-thick polystyrene films were probed by destabilization in an electric field. The non-cross-linked films showed the hallmark of viscoelasiticy; they exhibited elastic behavior at high shear rates and viscous rheology at low shear rates for stationary applied fields. These results are interpreted in terms of surface adhesion of chain segments in contact with the substrate surface, which substantially reduces reptative molecular motion of nearly all chains within the film.

DOI: 10.1103/PhysRevE.89.062604 PACS number(s): 82.35.Gh, 68.60.−p, 83.50.−v

## I. INTRODUCTION

Spin-cast polymer films are commonly used in polymer technologies and in the manufacture of many functional devices. While reasonably thick ($\gtrapprox$200 nm) polymer films are typically assumed to have polymer bulk behavior, thinner films often deviate from the bulk by showing a lowered glass transition temperature [1–6] and other anomalous dynamic behavior [7,8], which may stem from nonequilibrium polymer coil conformations [9–11]. Residual stresses in thin spin-cast films may cause their rupture and break-up [12–14], and in some instances bulk behavior can be restored by thermal and vapor annealing [10,15]. The study of these phenomena gives insight into the fundamental behavior of macromolecules in confinement and provides the basis for the predictable and controllable manufacture of thin films for a range of applications.

This study investigates a rheological transition as the thickness of thin high molecular weight polystyrene liquid films is reduced to dimensions below 100 nm. One method to measure the rheological properties of thin films is the analysis of the capillary wave spectrum [16,17]. Here the related electrohydrodynamic (EHD) film destabilization was used, where an electric field weakly perturbs the free surface of a liquid film [18].

## II. EXPERIMENT

Polystyrene (PS) with a very high weight-average molecular weight of 4060 kg mol$^{-1}$ (polydispersity: 1.15) was used as a model system. Here 44–192-nm-thick films were spin cast from filtered toluene (an athermal solvent for PS) at room temperature and trans-decalin (a $\Theta$ solvent for PS at $\sim 20\,^{\circ}$C) at 25 °C (termed TD25). All films were spun onto cleaned silicon substrates. To vary the substrate surface energy, the wafers were cleaned in an air plasma and by snow jetting, or covered with a hexamethyldisilazane (HMDS) self-assembled monolayer, resulting in highly polar and apolar substrates [19].

The experimental setup consisted of two almost parallel plates that formed a plate capacitor [Fig. 1(a)]. The PS films were spin cast onto the bottom plate, and SU8 spacers were deposited onto the top electrode to establish an air gap between both plates. The sandwiched PS-air films were placed into an oven, and the devices were heated to $T = 175\,^{\circ}$C, above the glass transition temperature $T_g$ of polystyrene. A small voltage ($\sim$40 V) was then applied, defining the start of the experiment. PS films were used as cast, after thermal annealing at $T = 155\,^{\circ}$C (ta) and after solvent-vapor annealing (va) for varying times. Vapor annealing was carried out in a sealed chamber filled with a controlled concentration of toluene vapor. The solvent vapor causes the polymer film to swell, enabling PS diffusion and thereby film equilibration, as described elsewhere [10,20]. The initial film thickness $h_0$ was determined by ellipsometry.

Film destabilization causes the formation of PS plugs that span the two electrodes [Fig. 1(b)]. After cooling the sandwiched system to room temperature and removal of the top plate, the capacitor spacing $d$ and wavelength $\lambda$ of the pattern that had formed were measured by atomic force microscopy [Fig. 1(b)]. A slight lateral variation in $d$ gave rise to a range of values of the electric field in the polymer $E_p$, allowing the acquisition of an entire data series from each sample. In some of the samples, the electrode-spanning PS plugs fractured when the electrodes were separated. In these cases, images from both electrodes were combined to a reliable measurement of $d$.

## III. THEORETICAL DESCRIPTION

### A. Viscous instability

The theory underpinning EHD instabilities in viscous films is described elsewhere [18,21]. Briefly, the surface of a liquid film is controlled by a force balance, where the destabilizing electrostatic pressure $p_{\mathrm{el}}$ is opposed by the stabilizing Laplace pressure $p_{\mathrm{L}}$. When $p_{\mathrm{el}}$ overcomes $p_{\mathrm{L}}$ an instability develops. From a linear stability analysis, the dominant instability wavelength is

$$\lambda = 2\pi \sqrt{\frac{\gamma U}{\epsilon_0 \epsilon_p (\epsilon_p - 1)^2}} E_p^{-\frac{3}{2}}, \tag{1}$$

where $\gamma$ is the surface tension, $U$ is the applied voltage, $\epsilon_0$ is the vacuum permittivity, $\epsilon_p$ is the dielectric constant of the

*Current address: Université Pierre & Marie Curie, 4 Place Jussieu, 75005 Paris, France.
†Current address: APS Editorial Office, Physical Review Letters, 1 Research Road, Ridge, New York 11961-2701, USA.
‡u.steiner@phy.cam.ac.uk

 

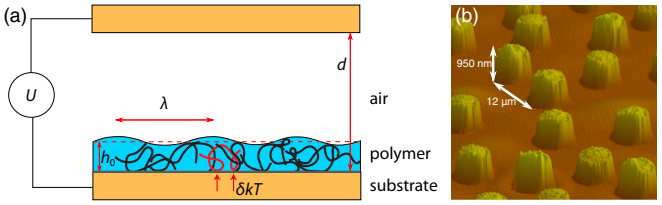


FIG. 1. (Color online) (a) Schematic drawing showing the experimental setup. Films of thickness $h_0$ were destabilized by applying a voltage $U$ to a capacitor with plate spacing $d$. Nearly all chains make contact with the substrate surface (indicated by arrows) and have an adhesive contact energy $\delta kT$. (b) EHD pattern measured by atomic force microscopy. The indicated dimensions were extracted from the AFM raw data.

polymer ($\epsilon_{PS} = 2.5$), and

$$E_p = \frac{U}{\epsilon_p d - (\epsilon_p - 1)h_0}. \quad (2)$$

Plotting $\lambda$ versus $E_p$ reveals the force balance at the polymer-air interface and allows additional contributions to the pressure balance acting on the surface of the polymer film to be identified. These include residual stresses $p_{res}$ arising from film preparation [10]. Note that the pattern morphology is determined by the early stage of the instability where the instability amplitude is much smaller than $\lambda$ and $h_0$, the so-called long wavelength limit for which Eq. (1) is valid. The validity of the predictions of Eq. (1) for the final morphologies shown in Fig. 1 has been confirmed by model calculations [22]. Note also that the values of $h$ and $d$ were chosen in such a way that pattern coarsening did not occur [23].

### B. Elastic instability

Rubber elastic thin films respond differently when exposed to an electric field. Rather than surface tension, the restoring force balancing the destabilizing dielectric pressure is the elastic modulus of the rubber [24]. In this case the most unstable wavelength is selected by the lowest elastic stiffness of the material, resulting in the simple scaling relation for the instability wavelength [25]

$$\lambda \approx 3h_0. \quad (3)$$

In contrast to Eq. (1), $\lambda$ is invariant to the nature and strength of the destabilizing force. While in thick films the restoring force exerted by surface tension is negligible compared to the elastic modulus $\mu$, this is not case for very thin films ($h_0 < 1$ μm). In the related case of film debonding driven by van der Waals forces, $\lambda/h_0$ is determined by the balance of the two restoring pressures [26]:

$$\frac{\lambda}{h_0} \approx 2\pi \left(\frac{\gamma}{3\mu h_0}\right)^{\frac{1}{4}}. \quad (4)$$

Unlike the electrohydrodynamic instabilities of liquid films, elastic films require a threshold destabilization pressure, i.e., a threshold applied voltage of [27,28]

$$U_c^2 = \frac{6.22\mu}{\epsilon_0 \epsilon_p (\epsilon_p - 1)^2} \frac{(\epsilon_p(d + h_0) + h_0)^3}{h_0}. \quad (5)$$

## IV. RESULTS AND DISCUSSION

### A. Film thickness dependence

To investigate the thickness dependence of the EHD instability, 44–192-nm-thick as-cast PS films were studied. The results are shown in Fig. 2. This range was chosen so that the lower limit was comparable to the radius of gyration of the chains of $R_g \approx 54$ nm, and the upper limit was 3.5 times this value. In sufficiently thick films ($h_0 \gg R_g$), the PS chains in the film should approach bulk behavior in terms of their molecular structure and their entanglements [29].

Three different qualitative regimes can be observed in Fig. 2. The data of the two thickest films ($h_0 \gtrsim 170$ nm) follow the prediction of Eq. (1) [Fig. 2(d)], indicating that the as-cast films were stress-free and no additional forces were acting on the films. In the intermediate thickness range of 100 nm $\lesssim h_0 \lesssim$ 150 nm [Fig. 2(c)], the data points lie predominantly above the line of Eq. (1). As described before in Refs. [9,10], this arises from a stabilizing, thin, visco-elastic surface layer ("crust") that is thought to form during rapid solvent evaporation [30] and provides an additional force aiding $p_L$. In these two regimes the $\lambda$ versus $E_p$ variation of the data follows closely the functional dependence of Eq. (1), up to high fields > 60 V/μm [10].

Interestingly, the opposite effect is observed in very thin films with $h_0 \lesssim 75$ nm [Fig. 2(a)]. Here the experimental data clearly lie below the predicted $\lambda$ versus $E_p$ variation for $E_p <$ 25 V/μm and above the predicted variation for larger $E_p$. The variation for 75 nm $\lesssim h_0 \lesssim$ 100 nm in Fig. 2(b) is less well defined with datasets lying on either side of the predicted curve. Clearly there is a marked change in the film instability as the film thickness approaches ~70 nm.

The behavior of PS films with intermediate thicknesses [Fig. 2(c)] has been discussed in detail before [10] and is due to PS coils that are quenched out of equilibrium during spin-coating, where the behavior strongly depends on the quality of the spin-coating solvent. When annealed for a sufficiently long time by heating, or in a solvent vapor atmosphere, the

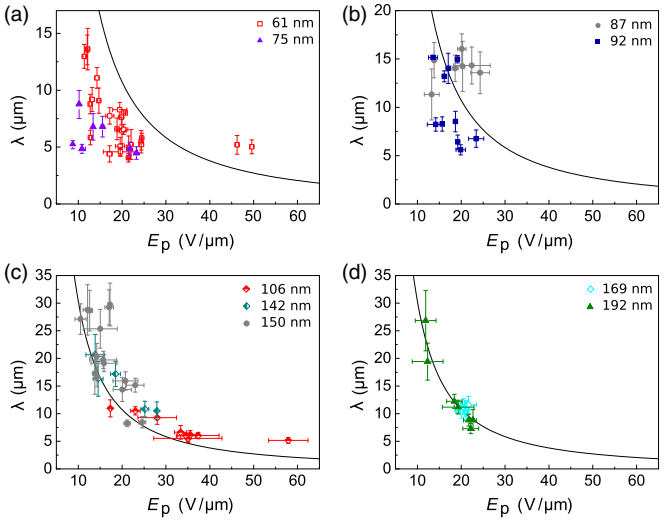


FIG. 2. (Color online) Electric field-induced instabilities in PS films as cast from toluene, with thicknesses ranging from 61 to 192 nm (inset). The solid lines are the prediction of Eq. (1).

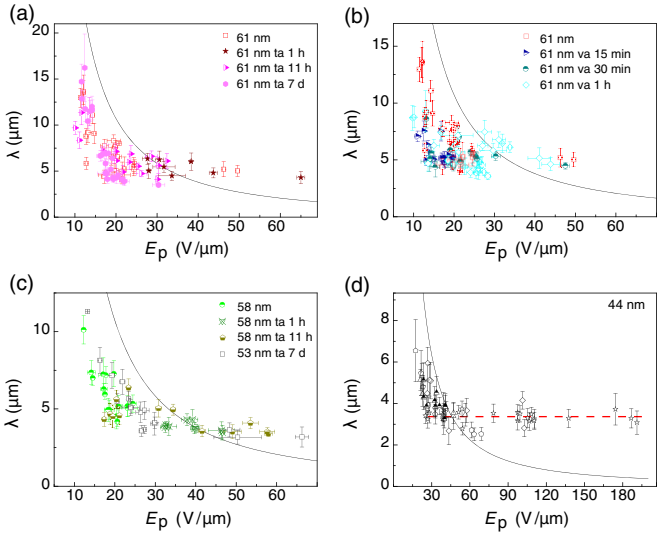


FIG. 3. (Color online) Annealing series of thin PS films. (a) Thermal and (b) vapor annealing of PS films cast from toluene. (c) Themal annealing of PS films cast from trans-decalin at 25 °C. (d) The five 44 nm thick films cast from toluene show the reproducability of the data. The solid lines are predictions from Eq. (1). The dashed line is a guide to the eye. Film thicknesses, annealing type and times are given in the insets.

PS chains equilibrate, leading to a rheological behavior of the films that is described by Eq. (1).

It is therefore interesting to investigate (1) whether the results of Fig. 2(a) vary when the spin-coating solvent is changed and (2) what effect thermal and solvent annealing have.

### B. Variation with spin-coating solvent and annealing

EHD instabilities of films cast from toluene and TD25 that were annealed for different length of time are shown in Fig. 3. In contrast to thicker films ($h_0 \gtrsim 100$ nm) where annealing leads to data series that fall onto the line predicted by Eq. (1) [9,10], the data of films with $h_0 \lesssim 60$ nm vary neither with the spin-coating solvent nor with the annealing time. This may indicate that an additional physical process overrides these earlier described phenomena of film preparation dependence.

Interestingly, the destabilization of these thin films is only weakly dependent on the destabilizing field for a wide range of $E_p$ values. However, below a critical value $E_c$ ($E_p \lesssim E_c$), λ is seen to strongly vary with $E_p$. The constant λ regime is indicated by the dashed line in Fig. 3(d). For $h_0 \approx 60$ nm, $E_c \approx 15$–$20$ V/μm, and for $h_0 = 44$ nm, $E_c \approx 30$ V/μm.

A nearly constant value of λ as a function of $E_p$ is not compatible with the theory of EHD of viscous liquid films, given by Eq. (1). The invariance of λ with $E_p$ in the $E_p > E_c$ regime is instead reminiscent of instabilities of elastomeric thin films given by Eq. (3). While the instability kinetics of very thin films exposed to electric fields is unexplored, we turn to the model of [26] that yields Eq. (4). The applicability of Eq. (4) for small values of $h$ is, however, questionable since the right-hand side of Eq. (4) diverges as $h \to 0$ for any given set of $\gamma$ and $\mu$.

The plateau λ values of the 61 nm, 58 nm, 53 nm, and 44 nm-thick films in the high-field constant regime are ≈4.4 μm, ≈3.8 μm, ≈3.6 μm, and ≈3.4 μm, respectively. This corresponds to $\lambda/h_0$ values of 72, 66, 68, and 77, respectively. These values are ∼25 times larger compared to the proportionality constant of Eq. (3).

Accepting the validity of Eq. (4), this corresponds to elastic moduli, of $\mu \approx 9$ Pa for the 61 nm films, $\mu \approx 14$ Pa for the 58 nm and 53 nm-thick films, and 10 Pa for the 44-nm-thick films (where $\gamma = 30$ mN/m for PS at 175 °C). Given the scatter in the data shown in Fig. 3, $\mu$ is on the order of 10 Pa in all films. This modulus, which lies much below that of an entangled polymer melt, is surprising and questions the applicability of Eq. (4) for this system.

While the derived value of $\mu$ is debatable, our results indicate that it is very low. This is supported by the prediction of Eq. (5). Using the experimentally applied voltage of ≈ 40 V requires a modulus of less than 100 Pa. Nevertheless, moduli below a few kPa are unlikely for any type of polymer, underlining the requirement for an improved model.

### C. Thin film viscoelasticity

Based on the qualitative variation of the data in Fig. 3, we interpret the EHD rheology in thin films in terms of both elastic and viscous behavior. While the constant λ regime is evidence for elastic behavior as explained above, a viscous regime is observed for $E_p \lesssim E_c$ causing the deformation of the film into an array of plugs spanning the two electrodes [Fig. 1(b)]. In terms of this model the $\lesssim$60 nm films exhibit viscoelastic behavior; they respond elastically to high shear-rate perturbations and are viscous at low-shear rates or for static pressures that are applied for long enough times.

The characteristic film thickness of $h_0 \sim 60$ nm for this rheological behavior is interesting. It is close to $R_g = 55$ nm, and it is comparable to the thickness for which a much debated rheological anomaly sets in, the reduction of the glass transition temperature in thin films [31]. Since our experiments were carried out much above $T_g$, a correlation with the latter effect is unlikely.

In the absence of polymer-polymer cross-links and in the absence of viscoelasticity for thick films ($h_0 \gtrsim 100$ nm), the viscoelastic properties of the thin films are likely to arise from interactions between chain segments and the substrate. Silicon oxide-covered silicon wafers are high-energy surfaces to which polymer segments adhere [32]. For $h_0 \sim R_g$, segments in nearly every polymer chain in the film makes contact with the substrate [Fig. 1(a)]. Adhesive energies $\delta kT$ with $\delta > 1$ immobilize the segments and arrest chain motion by reptation, giving rise to a permanently elastic film. Contacts with $\delta < 1$ dramatically slow down chain relaxation, giving rise to viscoelasticity: a film of surface attached chains should respond elastically to high shear-rate perturbations and flow viscously when exposed to low-enough shear rates and in pressure gradients that are applied for long enough times.

Weak interfacial chain adsorption is able to account for the data of Fig. 3. From Ref. [33] we know that the characteristic response time varies with the applied electric field as $\tau \sim$

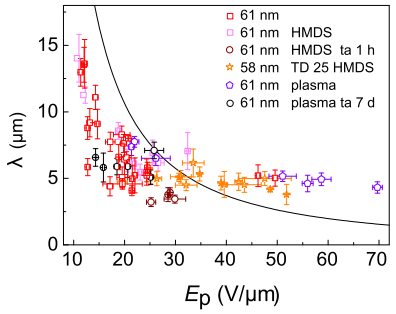


FIG. 4. (Color online) Wavelength of electric-field instabilitites in PS films on different substrates. Apolar surfaces were created by a HMDS self-assmbled monolayer, while surface polarity was increased by plasma etching. With the exception of TD25 (trans-decalin at 25 °C), all films were cast from toluene. Inset: thicknesses, substrate treatments, and annealing times.

$E_p^{-6}$ in the case of viscous instabilities. This gives rise to a substantial variation in the shear rates applied to the film with increasing $E_p$ and may cause elastic and viscous responses for high and low $E_p$, respectively. In the high $E_p$ regime, λ is set according to Eq. (4). The continued applied stress causes the flow of the polymer into a columnar pattern [Fig. 1(b)], the lateral length scale of which is determined by the initial elastic instability.

The existence of a $R_g$-thick layer of reduced mobility for thin films also has consequences on the relaxation of thicker films. We have previously shown that 100-nm-thick PS films with the molecular weight used here have an extrapolated equilibration time of tens of years, much longer than the reptation time of the polymer of ≈8 h at 175 °C [10]. The lack of equilibration of the 50–60-nm-thick films for annealing times up to 1 week suggests that a nearly immobilized layer at the substrate may be the cause for the slow relaxation rates seen in thicker films.

### D. The substrate boundary

Our model of thin-film viscoelasticity hinges on a moderate interactions of the chain segments with the high energy substrate surface. It is therefore interesting to investigate how substrate modification affects the EHD result. While highly slippery surfaces can be created by covering the silicon wafer with a thin cross-linked polydimethylsiloxane layer [12], very thin PS films spin cast onto these surfaces are highly unstable and dewet before the onset of an EHD-driven instability. Instead, the silicon wafers were covered by a self-assembled HMDS layer, allowing PS-film deposition and EHD destabilization of the film. Figure 4 shows the results for films deposited onto modified substrates. These results are the same as those shown in Fig. 3. While the results on slippery surfaces may seem surprising, they are in agreement with predictions of Brochard and de Gennes [34] and subsequent experimental results [35] that show that defects in the HMDS layer (possibly aided by the onset of HMDS thermal decomposition) lead to the formation of anchor chains that suppress slippage at low enough shear rates. These anchor chains would also suppress the viscous EHD response as indicated in the experiments shown in Fig. 4. While it is impossible to carry out the EHD experiment on very slippery films, enhancing interactions by cross-linking chains to the substrate may be a way corroborate this hypothesis [36].

## V. CONCLUSIONS

In conclusion, polystyrene films with thicknesses comparable to the polymer coil size show clear signs of viscoelasticity when destabilized in an electric field: they behave elastically at high electric fields (i.e., at sufficiently high shear rates) and exhibit viscous flow at low-shear rates and for stationary applied pressure gradients. In the absence of any other plausible mechanism, the elastic behavior is most likely due to segmental interactions with the substrate. An interaction strength $\delta kT$ with $\delta < 1$ is expected to cause high-shear rate elasticity, while enabling viscous flow on sufficiently long time scales.

The derived modulus of tens of Pa is surprisingly low since the entangled nature of high molecular weight PS should yield an intrinsic modulus on the order of 100 kPa [37]. While an improvement of the model leading to Eq. (4) may be required to arrive at a quantitative value of the modulus, our experimental results point to a low, finite elastic modulus in thin high $M_w$ PS films. Such a low modulus may be indicative of a strong reduction of entanglements in very thin spin cast films, as found before [10,29], particularly in the top-few nanometers of the film that set the lateral length scale during the early stage of the EHD film instability.

Beyond the model calculations used to interpret the data, the experimentally observed viscoelastic effect is remarkably robust. It is invariant to the nature of the substrate surface, film preparation procedures, and annealing protocols. It is therefore likely that this behavior is important in polymer films with thicknesses comparable to the radius of gyration of the chains and strong adhesive interactions with the substrate.

## ACKNOWLEDGMENTS

We acknowledge the support from the Winton Programme for the Physics of Sustainability.

[1] J. L. Keddie, R. A. L. Jones, and R. A. Cory, Europhys. Lett. **27**, 59 (1994).
[2] Z. Fakhraai, S. Valadkhan, and J. Forrest, Eur. Phys. J. E **18**, 143 (2005).
[3] J. E. Pye and C. B. Roth, Phys. Rev. Lett. **107**, 235701 (2011).
[4] O. Bäumchen, J. D. McGraw, J. A. Forrest, and K. Dalnoki-Veress, Phys. Rev. Lett. **109**, 055701 (2012).
[5] B. J. Gurmessa and A. B. Croll, Phys. Rev. Lett. **110**, 074301 (2013).
[6] D. Cangialosi, V. M. Boucher, A. Alegría, and J. Colmenero, Phys. Rev. Lett. **111**, 095701 (2013).
[7] H. Bodiguel and C. Fretigny, Phys. Rev. Lett. **97**, 266105 (2006).
[8] T. Kanaya, T. Miyazaki, R. Inoue, and K. Nishida, Phys. Status Solidi B **242**, 595 (2005).

[9] D. R. Barbero and U. Steiner, Phys. Rev. Lett. **102**, 248303 (2009).
[10] K. R. Thomas, A. Chenneviere, G. Reiter, and U. Steiner, Phys. Rev. E **83**, 021804 (2011).
[11] A. Raegen, M. Chowdhury, C. Calers, A. Schmatulla, U. Steiner, and G. Reiter, Phys. Rev. Lett. **105**, 227801 (2010).
[12] G. Reiter, M. Hamieh, P. Damman, S. Sclavons, S. Gabriele, T. Vilmin, and E. Raphaël, Nat. Mater. **4**, 754 (2005).
[13] P. Damman, S. Gabriele, S. Coppée, S. Desprez, D. Villers, T. Vilmin, E. Raphaël, M. Hamieh, S. Al Akhrass, and G. Reiter, Phys. Rev. Lett. **99**, 036101 (2007).
[14] A. Clough, M. Chowdhury, K. Jahanshahi, G. Reiter, and O. K. C. Tsui, Macromolecules **45**, 6196 (2012).
[15] R. L. Jones, S. K. Kumar, D. L. Ho, R. M. Briber, and T. P. Russell, Nature (London) **400**, 146 (1999).
[16] Z. Yang, Y. Fujii, F. K. Lee, C.-H. Lam, and O. K. C. Tsui, Science **328**, 1676 (2010).
[17] Z. Yang, A. Clough, C.-H. Lam, and O. K. C. Tsui, Macromolecules **44**, 8294 (2011).
[18] E. Schäffer, T. Thurn-Albrecht, T. P. Russell, and U. Steiner, Nature (London) **403**, 874 (2000).
[19] E. Vansant, P. Van Der Voort, and K. Vrancken, *Characterization and Chemical Modification of the Silica Surface* (Elsevier, Amsterdam, 1995).
[20] S. Hüttner, M. Sommer, A. Chiche, G. Krausch, U. Steiner, and M. Thelakkat, Soft Matter **5**, 4206 (2009).
[21] E. Schäffer, T. Thurn-Albrecht, T. P. Russell, and U. Steiner, Europhys. Lett. **53**, 518 (2001).
[22] L. F. Pease, III and W. B. Russel, Langmuir **20**, 795 (2004).
[23] N. Voicu, S. Harkema, and U. Steiner, Adv. Funct. Mater. **16**, 926 (2006).
[24] J. Sarkar, A. Sharma, and V. B. Shenoy, Phys. Rev. E **77**, 031604 (2008).
[25] N. Arun, A. Sharma, V. Shenoy, and K. Narayan, Adv. Mater. **18**, 660 (2006).
[26] M. Gonuguntla, A. Sharma, J. Sarkar, S. A. Subramanian, M. Ghosh, and V. Shenoy, Phys. Rev. Lett. **97**, 018303 (2006).
[27] N. Arun, A. Sharma, P. S. G. Pattader, I. Banerjee, H. M. Dixit, and K. S. Narayan, Phys. Rev. Lett. **102**, 254502 (2009).
[28] J. Sarkar and A. Sharma, Langmuir **26**, 8464 (2010).
[29] L. Si, M. V. Massa, K. Dalnoki-Veress, H. R. Brown, and R. A. L. Jones, Phys. Rev. Lett. **94**, 127801 (2005).
[30] P. G. de Gennes, Eur. Phys. J. E **7**, 31 (2002).
[31] C. J. Ellison, M. K. Mundra, and J. M. Torkelson, Macromolecules **38**, 1767 (2005).
[32] P. T. Wilson, L. J. Richter, W. E. Wallace, K. A. Briggman, and J. C. Stephenson, Chem. Phys. Lett. **363**, 161 (2002).
[33] P. Goldberg-Oppenheimer and U. Steiner, Small **6**, 1248 (2010).
[34] F. Brochard and P. G. De Gennes, Langmuir **8**, 3033 (1992).
[35] K. B. Migler, H. Hervet, and L. Léger, Phys. Rev. Lett. **70**, 287 (1993).
[36] R. S. Tate, D. S. Fryer, S. Pasqualini, M. F. Montague, J. J. de Pablo, and P. F. Nealey, J. Chem. Phys. **115**, 9982 (2001).
[37] M. Rubinstein and R. H. Colby, *Polymer Physics* (Oxford University Press, Oxford, 2003).